



Contents lists available at ScienceDirect

Journal of Advanced Research

journal homepage: www.elsevier.com/locate/jare

Exploitation of enhanced prime editing for blocking aberrant angiogenesis

Xionggao Huang^{a,#}, Wenyi Wu^{b,#}, Hui Qi^{c,#}, Xiaohe Yan^c, Lijun Dong^c, Yanhui Yang^d, Qing Zhang^e, Gaoen Ma^{a,e,*}, Guoming Zhang^{c,**}, Hetian Lei^{f,***}

^a Department of Ophthalmology, The First Affiliated Hospital of Hainan Medical University, Haikou, China

^b Department of Ophthalmology, Hunan Key Laboratory of Ophthalmology, Xiangya Hospital, Central South University, Changsha, China

^c Shenzhen Eye Hospital, Jinan University, Shenzhen Eye Institute, Shenzhen, China

^d Ningxia Key Laboratory of Prevention and Control of Common Infectious Diseases, the School of Basic Medical Sciences, Ningxia Medical University, Yinchuan, China

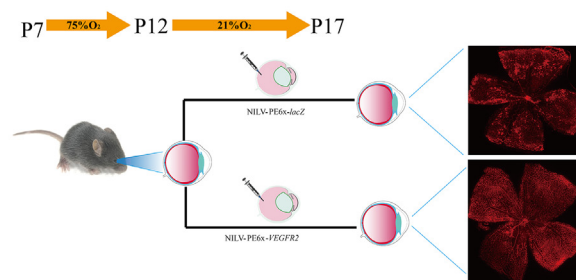
^e Department of Ophthalmology, The Third Affiliated Hospital of Xinxiang Medical University, Xinxiang, China

^f Department of Ophthalmology, Shanxi Bethune Hospital, Shanxi Academy of Medical Sciences, Third Hospital of Shanxi Medical University, Tongji Shanxi Hospital, Taiyuan, China

HIGHLIGHTS

- Establishment of a novel prime editing (PE)6x system.
- Creation of a dominant negative (DN) VEGFR2 with dual non-integrating lentivirus (NILV)-mediated PE6x.
- Prevention of VEGF-induced VEGFR2 activation by PE6x-created DN-VEGFR2 *in vitro* and *in vivo*.
- Inhibition of pathological retinal angiogenesis by PE6x-generated DN-VEGFR2 in a mouse model of oxygen-induced retinopathy.

GRAPHICAL ABSTRACT



Prime editing inhibits retinal angiogenesis

ARTICLE INFO

Article history:

Received 2 September 2023

Revised 26 January 2024

Accepted 7 July 2024

Available online xxxx

Keywords:

Enhanced prime editing

Dominant-negative VEGFR2

Angiogenesis

Oxygen-induced retinopathy

ABSTRACT

Introduction: Aberrant angiogenesis plays an important part in the development of a variety of human diseases including proliferative diabetic retinopathy, with which there are still numerous patients remaining a therapeutically challenging condition. Prime editing (PE) is a versatile gene editing approach, which offers a novel opportunity to genetically correct challenging disorders.

Objectives: The goal of this study was to create a dominant-negative (DN) vascular endothelial growth factor receptor (VEGFR) 2 by editing genomic DNA with an advanced PE system to block aberrant retinal angiogenesis in a mouse model of oxygen-induced retinopathy.

Methods: An advanced PE system (referred to as PE6x) was established within two lentiviral vectors, with one carrying an enhanced PE guide RNA and a canonical Cas9 nickase fused with an optimized reversal transcriptase, and the other conveying a nicking guide RNA and a DN-MLH1 to improve PE efficiency. Dual non-integrating lentiviruses (NILVs) produced with the two lentiviral PE6x vectors were then employed to create a mutation of *VEGFR2* T17967A by editing the *Mus musculus VEGFR2* locus *in vitro*

* Corresponding author at: 3 Xueyuan Road, the First Affiliated Hospital of Hainan Medical University, Haikou 570102, China.

** Corresponding author at: 18 Zetian Road, Shenzhen Eye Hospital, Shenzhen, 518000, China.

*** Corresponding author at: N99 Longcheng street, Shanxi Bethune Hospital, Taiyuan, 030032, China.

E-mail addresses: 15757826611@163.com (G. Ma), 3823509060@163.com (G. Zhang), leihetian18@hotmail.com (H. Lei).

These authors made equal contributions to these work.

<https://doi.org/10.1016/j.jare.2024.07.006>

2090-1232/© 2024 The Authors. Published by Elsevier B.V. on behalf of Cairo University.

This is an open access article under the CC BY-NC-ND license (<http://creativecommons.org/licenses/by-nc-nd/4.0/>).

and *in vivo*, leading to generation of a premature stop codon (TAG, K796^{stop}) to produce DN-VEGFR2, to interfere with the wild type VEGFR2 which is essential for angiogenesis.

Results: NILVs targeting *VEGFR2* delivered into cultured murine vascular endothelial cells led to 51.06 % *VEGFR2* T17967A in the genome analyzed by next generation sequencing and the production of DN-VEGFR2, which was found to hamper VEGF-induced VEGFR2 phosphorylation, as demonstrated by Western blot analysis. Intravitreally injection of the dual NILVs into postnatal day 12 mice in a model of oxygen-induced retinopathy, led to production of retinal DN-VEGFR2 in postnatal day 17 mice which blocked retinal VEGFR2 expression and activation as well as abnormal retinal angiogenesis without interfering with retinal structure and function, as assessed by electroretinography, optical coherence tomography, fundus fluorescein angiography and histology.

Conclusion: DN-VEGFR2 resulted from editing genomic *VEGFR2* using the PE6x system can be harnessed to treat intraocular pathological angiogenesis.

© 2024 The Authors. Published by Elsevier B.V. on behalf of Cairo University. This is an open access article under the CC BY-NC-ND license (<http://creativecommons.org/licenses/by-nc-nd/4.0/>).

Introduction

Angiogenesis, a process by which new blood vessels sprout from pre-existing vessels [1–3], is associated with a variety of human diseases including proliferative diabetic retinopathy (PDR) [4,5], retinopathy of prematurity (ROP) [6], and neovascular age-related macular degeneration (nAMD) [7,8]. The signaling pathway of vascular endothelial growth factor (VEGF)/VEGF receptor (VEGFR)2 is essential for angiogenesis [9–12], and thus a number of antagonists such as ranibizumab, bevacizumab, and aflibercept, interrupting this pathway, have been developed for treating angiogenesis-associated human diseases [13–17]. Nevertheless, there are still myriad patients with these diseases resistant to such therapies [16–18]. Thereby, novel therapeutic approaches are urgently needed to angiogenesis-associated diseases including PDR, which occupies the highest number of acquired blindness in the working-age people [4,5].

Genome editing provides novel therapeutic opportunities for human diseases that are currently challenging for therapy [19,20]. Prime editing (PE) is a versatile gene editing system which consists of at least two components: a Cas9 nickase (n) including *Streptococcus pyogenes* (Sp) Cas9H840A(Cas9n) fused with an engineered reverse transcriptase (RT) (the PE1 protein) and a prime editing guide RNA (pegRNA). This pegRNA is composed of a single guide (sg) RNA and a 3' extension with a primer binding sequence (PBS) that is complementary to a portion of the DNA protospacer, and a RT template that contains the desired mutation(s) [21]. The pegRNA function can be much improved by fusion with a structured RNA motif such as tevopreQ₁ (trimmed evopreQ₁) to its 3'-terminus to enhance its stability and protection from degradation designated as an enhanced (e) pegRNA [22], whereas the RT can be codon-optimized with D200N/L603W/T330P/T306K/W313F to improve PE1 activity, referred to as PE2 [21]. Thereby, an epegRNA can guide the Cas9n-RT complex to bind one strand of a target DNA locus and to nick the opposite strand with a protospacer adjacent motif (PAM), resulting in exposure of a DNA end for the PBS to prime RT to reversely transcribe the RT template. As a consequence, the desired mutation(s) in the RT template are incorporated into the targeted genomic locus [23].

PE2 efficiency can be further improved to PE3 by using an additional sgRNA to direct Cas9n to nick the non-edited strand at a location about 50 base pair (bp) away from the pegRNA target [21]. Specific DNA mismatch repair (MMR) genes have been discovered that strongly suppress PE efficiency and promote formation of insertion/deletions (indels). To this end, co-expression of a dominant negative MMR protein (MLH1dn) with PE2 designated as PE4 or with PE3 as PE5 has been developed to further improve PE efficiency. In addition, synergizing with PE4, PE5 and epegRNAs, optimized prime editors including PE6a-g can further raise PE efficiency [24,25]. Moreover, a truncated RT has also been demonstrated to

be capable of enhancing PE efficiency [26]. To date, PE has been broadly applied to introduce genetic changes in a variety of animal models including flies [27], zebrafish [28], and mice [19,25,29–33].

Adeno-associated virus (AAV) is the most frequently used vector for *in vivo* gene editing due to its non-pathogenic, low immune response and sustained-expression in non-dividing cells [34,35]. Nevertheless, in the clinical scenario, it would be ideal to have a gene editing system expressed transiently (hit-and-run) to reduce potentially detrimental effects. A non-integrating lentiviral vector (NILV) fits this purpose very well. The NILV system can be achieved by following approaches: (1) inactivating integrase by mutation of any amino acid of its catalytic triad (D64, D116, and E152) [36] or replacement of the ²⁶²RRK motif with AAH [37]; (2) altering the integrase-recognition sequences (att) in the viral LTR (long-term repeats) [38]; and (3) ruining the active center of RT by changing the amino acid sequence YMDD to YMVV [39]. Such a NILV vector has the advantage of being able to accommodate up to 8 kilobases (kb) of nucleotides of interest compared to an AAV vector, which has a 4.7-kb package limitation [37].

Genome editing other than PE has been leveraged to prevention of intraocular angiogenesis in animal models [40–43]. In comparison to other gene editing technologies, PE can precisely achieve all types of desired mutations in the genomic DNA of living cells including base pair substitutions, small insertion/deletions (indels) without requiring either a double-strand DNA break (DSB) or a foreign DNA template [44]; however, while this strategy has been harnessed to install or correct mutations in a number of mouse models [19,25,29–33,45,46], whether this strategy can be harnessed for preventing pathological retinal angiogenesis has not yet been explored.

The goal of this study was to create a dominant negative (DN) VEGFR2 by editing genomic DNA with an advanced PE system to block aberrant retinal angiogenesis in a mouse model of oxygen-induced retinopathy (OIR) [40,47–49]. To achieve this aim, we designed a dual NILV system with a D64V mutation in integrase [50] carrying LTR-EF1 α -SpCas9n-RT-U6-epegRNA-LTR (LV5) and LTR-EF1 α -MLH1dn-U6-nicking sgRNA-LTR (LV6) (termed as PE6x) targeting genomic *VEGFR2* (Figure: Fig. 1), which would be delivered intravitreally to mice in the mouse OIR model [40,47,48] to suppress hypoxia-induced retinal angiogenesis.

Materials and methods

Major reagents

Primary antibodies against VEGFR2 (Catalog #: 9698), and p-VEGFR2 (Y996) (Catalog #: 2474) were purchased from Cell Signaling Technology (Danvers, MA, USA); in addition, an antibody against VEGFR2 N-terminal (Catalog #: BS-10412R) was bought from

A. Schematic of dual integrase-deficient lentiviruses delivering PE6x

1) Lenti-EF-1-SpCas9n-RT-U6-epgRNA(LV5)

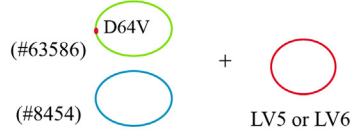


2) Lenti-EF-1-MLH1dn-U6-sgRNA(nicking)(LV6)



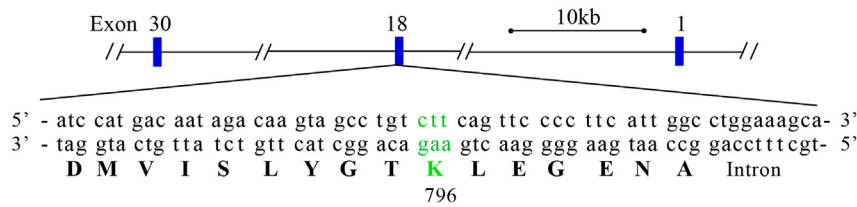
3) An integrase deficient packaging vector (#63586)

4) A VSV-G vector (#8454)

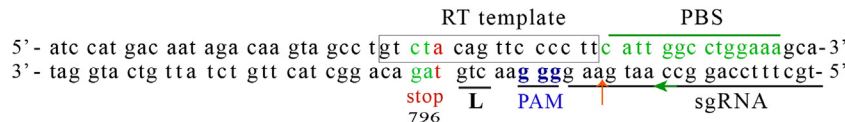


B. Schematic of generating a mutant of VEGFR2 (K796stop) with PE6x

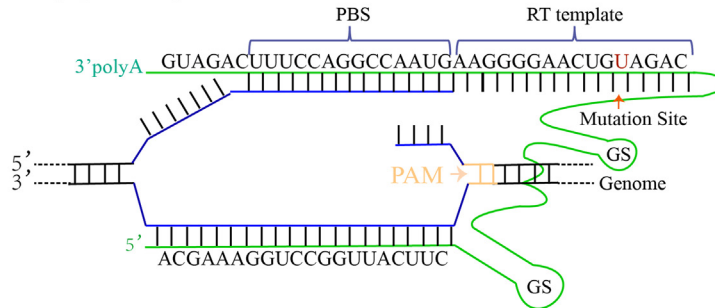
1) A Mus musculus VEGFR2 locus (NC_000071.6)



2) Schematic of creating VEGFR2 T17967A(K796stop) using PE6x



3) The epegRNA sequence



C. Schematic of the dominant negative VEGFR2

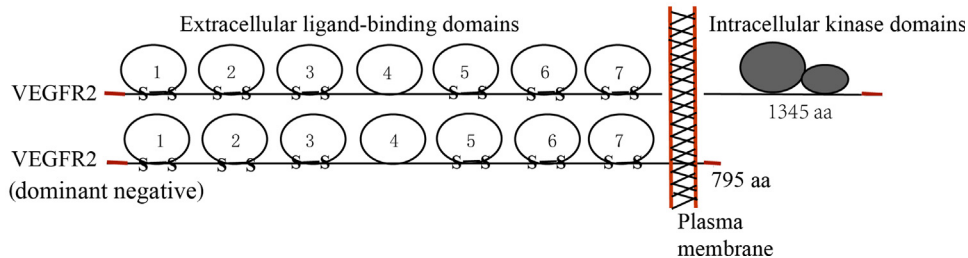


Fig. 1. Schematic of generating dominant-negative VEGFR2 with prime editing **A.** Schematic of dual integrase-deficient lentiviruses delivering PE6x **1)** A lentiviral vector (LV5) carrying DNA sequences for a fusion protein of SpCas9n (H840A) with RT (enhanced codon optimized reverse transcriptase) driven by a promoter of EF (elongation factor)-1 α and U6-epgRNA. U6: U6 promoter, LTR: long terminal repeat. **2)** A lentiviral vector (LV6) carrying EF-1 α -MLH1dn and U6-sgRNA for nicking (ngRNA). MLH1dn: MLH1 dominant negative. **3-4)** Plasmids of an integrase-deficient packaging vector with a mutation D64V (Catalog #: 63586, Addgene), a vector expressing lentiviral envelope (Catalog #: 8454, Addgene), and LV5 or LV6 were transfected into 293 T cells for production of integrase-deficient lentiviruses (LV5 or LV6). VSV-G: vesicular stomatitis virus-G protein. **B.** Schematic of generating a dominant negative VEGFR2 (K796stop) with PE6x **1)** Schematic of a *Mus musculus* VEGFR2 locus (NC_000071.6) showing the 796th amino acid lysine (K) for mutation. **2)** Schematic of creating VEGFR2 T17967A (K796stop) using PE6x RT template (16 nucleotides: nt): template for reverse transcription, PBS (14 nt): primer binding sequence, PAM: protospacer adjacent motif, a protospacer sequence for generating a sgRNA, PBS: primer binding site. **3)** An epegRNA sequence for generating VEGFR2 T17967A (K796stop) using PE6x. tevopreQ1: truncated evopreQ1 sequence for protection of epegRNA from degradation. **C.** Schematic of the full and dominant negative VEGFR2 Full VEGFR2 (1345aa): an extracellular domain for ligand binding with 7 IgG domains linked by intra S-S bonds, a plasma membrane domain for crossing plasma membrane, and an intracellular domain with kinase domains; dominant negative (DN) VEGFR2 (795aa) with a mutation (K796stop) at intracellular juxtamembrane.

Thermo Fisher Scientific (Waltham, MA, USA), and one against β -Actin (Catalog #: sc-47778) was purchased from Santa Cruz Biotechnology (Santa Cruz, CA, USA). Horseradish peroxidase (HRP)-conjugated goat anti-rabbit IgG and anti-mouse IgG were ordered from Santa Cruz Biotechnology. Enhanced chemiluminescent substrate for detection of HRP and Alexa fluorescence-594-conjugated mouse endothelial specific isolectin B4 (IB4) were purchased from Thermo Fisher Scientific. High-fidelity Herculase II DNA polymerases were from Agilent Technologies (Santa Clara, CA, USA).

DNA constructs

DNA sequences (TGCTTCCAGGCCAATGAAGGTTTTAGAGCTAG AATAGCAAGTTAAAATAAGGCTAGTCCGTTATCAACTTGAAAAAGT GGCACCGAGTCGGTGGCTCTACAGTTCCC CTTCATTGGCCTGGAAAgc aCGCGTTCTATCTAGTTACGCGTTAAACCACTAGAAAtttt. Spacer: T GCTTCCAGGCCAATGAAG, Scaffold: GTTTTAGAGCTAGAAATAGC AAGTAAA ATAAGGCTAGTCCGTTATCAACTTGAAAAAGTGGCACC G AGTCGGTGC, RT template: GTCTACAGTTCCTT, PBS: CATTGG CCTGGAAA, linker: gca, 3 motif: CGCGTTCTATCTAGTTACGCGT TAAACCACTAGAA, terminator: tttttt) (named VXPEG1) and TCATCCAAGGGCA ATTCATC (named VX1) in the mouse *VEGFR2* genomic locus (NC_000071.6) (Table 1) were selected for generating enhanced prime editing single guide RNA (epegRNA) and nicking guide (ng)RNA for SpCas9 nickase (n) based on previous publications [22,51,52]. The control spacer sequence (5-TGCGAATACGCCACGC GATGGG -3) from the *lacZ* gene of *Escherichia coli* was designed for control epegRNA and nicking sgRNA [22,51,53–55].

The pLTR- EF1-SpCas9n (H840A)-eRT- U6-epegRNA-LTR (LV5) was derived from lent-crispr v2- (Cat. 52961, Addgene, Cambridge, MA, USA) [56] by replacing SpCas9 with SpCas9n (H840A)-eRT [21] and then inserting synthesized epegRNA; The pLTR- EF1-MLH1dn-U6-sgRNA-LTR (LV6) was also derived from lenti-crispr v2 by replacing SpCas9 with MLH1dn [21,24] and then inserting a ngRNA by *BsmB1*. All these constructs were confirmed by DNA sequencing.

To construct ngRNA, the top oligo 5 CACCG- TCATCCAAGGG- CAATTCATC) and bottom oligo: 5-AAAC-20nt-C-3(20nt: complimentary top oligo sequences) were annealed and cloned into the LV6 vector by *BsmB1*. All clones were confirmed by DNA sequencing using a primer 5-GGACTATCATATGCTTACCG-3 from the sequence of U6 promoter driving expression of gRNAs. Both synthesis of oligos and Sanger DNA sequencing were performed by Tsingke Biotechnology Co., Ltd (Guangzhou, China).

Cell culture

Human embryonic kidney (HEK) 293 T cells (containing SV40 T-antigen) from America Type Culture Collection (ATCC, Manassas,

VA, USA) were cultured in high-glucose (4.5 g/L) DMEM supplemented with 10 % FBS. C57BL/6 mouse primary brain microvascular endothelial cells (MVECs) were purchased from CellBiologics (Chicago, IL, USA) and cultured in the endothelial cell medium with a kit (CellBiologics). All cells were cultured at 37 °C in the humidified atmosphere with 5 % CO₂ [40,57,58].

Production of lentivirus and non-integrating lentivirus

A lentiviral vector (LV5 or LV6, 28 μ g), a lentiviral envelope plasmid VSV-G (Catalog #: 8454, Addgene) (7 μ g) [59], and a lentiviral packaging plasmid *psPAX2* (Catalog #: 12260, Addgene) (21 μ g) or an integrase-deficient lentiviral packaging vector (21 μ g) (Catalog #: 63586, Addgene) [50] were mixed together in DMEM without phenol (2 ml), and then a polyethylenimine (PEI) solution (220 μ l, 1 μ g/ μ l, PolySciences: #23966-2, IL, USA) was added to the mixtures. After thoroughly mixed, they were incubated at room temperature for 15 min and then respectively transferred into a 150-mm cell culture dish with HEK 293 T cells, which were approximately 70 % confluent without antibiotics. After 18 h (37 °C, 5 % CO₂), the medium was replaced with a fresh culture medium. At 24 h after changing the medium, lentiviruses were firstly harvested, and the viral harvest was repeated at 24-h intervals for 3 times. The virus-containing media were pooled and centrifuged at 800 \times g for 5 min; the supernatants were then subjected to a centrifugation at 25,000 \times g for 90 min at 4 °C. Finally, the viral pellets were re-suspended in 500 μ l of sterile TNE buffer (50 mM Tris pH 7.8, 130 mM NaCl, 1 mM EDTA), which were then transferred into microtubes, and dissolved at 4 °C with gentle rotation overnight. These dissolved lentiviruses were then titrated [60,61] to infect MVECs in the presence of 8 μ g/ml polybrene or kept at -80 °C [54,55,57,62].

Transduction of vascular endothelial cells in vitro

Culture media of MVECs at 80 % confluence in 6-well plates were changed into the fresh culture, followed by addition of lentiviruses or NILVs [10 μ l/well, 5 \times 10⁹ viral genome-containing particles (vg)/ml] to the culture media supplemented with an additional 8 μ g/ml polybrene. At desired periods after infection, the cells were harvested in 1 \times extraction buffer (EB, 10 mM Tris-HCl, pH 7.4, 5 mM EDTA, 50 mM NaCl, 50 mM NaF, 1 % Triton X-100, 20 μ g/ml aprotinin, 2 mM Na₃VO₄, and 1 mM phenylmethylsulfonyl fluoride) for Western blotting analysis, or in lysis buffer for isolation of genomic DNA [54,55,57,62].

Table 1
Selection of epegRNA for editing mouse *VEGFR2*.

epegRNA		Sequences
1	sgRNA RT template (16nt) PBS (14 nt)	TGCTTCCAGGCCAATGAAG GTCTACAGTTCCTT CATTGGCCTGGAAA
2	sgRNA RT template PBS	TATGCTTCCAGGCCAATGA TCTACAGTTCCTT CATTGGCCTGGAAAGC
3	sgRNA RT template PBS	GGGGAGGATTTATGCTTCC TGCTACAGTTCCTT CATTGGCCTGGAAAG
EvopreQ1 ngRNA		CGCGTTCTATCTAGTTACGCGTTAAACCACTAGAA TCATCCAAGGGCAATTCATC
PCR primers	P51F P51R	GCCAGATGAGCGGTA TGAGATTATCATGAATGAGCC

Western blotting

When infected MVECs reached 90 % confluence, they were deprived of growth factors for 16 h, followed by treatment with or without VEGF (10 ng/ml) for 10 min. The cells were collected in 1 × EB and their protein concentrations in the EB were determined using a BCA protein assay kit (Thermo Fisher Scientific).

Proteins in the EB were then resolved in the 5 × protein sample buffer [25 mM EDTA (pH = 7.0), 10 % sodium dodecyl sulfate (SDS), 500 mM dithiothreitol, 50 % sucrose, 500 mM Tris HCl (pH 6.8), and 0.5 % bromophenol blue], and subjected to 10 % SDS-polyacrylamide gel electrophoresis (PAGE). Proteins in the gel were transferred to polyvinylidene difluoride (PVDF) membranes and subjected to western blot analysis using desired antibodies. Experiments were repeated at least three times. Signal intensity was determined by densitometry using NIH ImageJ software (USA) [54,55,57,62].

DNA sequencing

MVECs or mouse retinas were collected for genomic DNA extraction according to the manufacturer's protocol of the Quick-Extract DNA Extraction from Epicenter (Chicago, IL, USA). Briefly, the cell pellets were re-suspended in the QuickExtract solution, vortexed, and incubated at 65 °C for 6 min; the lysates were vortexed again and then incubated at 100 °C for 10 min. DNA fragments from a mouse *VEGFR2* genomic locus with the anticipated mutation were PCR amplified with high-fidelity Herculase II DNA polymerases. Primers named as P51 were (forward P51F: 5-AGCCAGATGAGCGG GTAAAA-3), and (reverse P51R: 5-TGAGATTAT CATGAATGAGGCC-3). The PCR products were separated in 2 % agarose gel and purified with a gel extraction kit (Thermo Fisher Scientific) for Sanger DNA sequencing and next generation sequencing (NGS). Primer synthesis and DNA sequencing were conducted by Tsingke Biotechnology Co., Ltd.

Transduction of vascular endothelial cells in vivo

NILVs for *in vivo* use were produced by Shandong Vigene Biosciences, Inc. (Jinan, China). Briefly, lentiviral vectors including pLTR-EF1-SpCas9n (H840A)-eRT- U6-pegRNA-LTR (LV5), pLTR-EF1-MLH1dn-U6-sgRNA-LTR (LV6) and pLTR-EF1-EGFP-LTR, respectively with a vector expressing a lentiviral envelope protein (Catalog #: 8454, Addgene) [59] and a integrase-deficient lentiviral packaging vector (Catalog #: 63586, Addgene) [50] were transfected into HEK293T cells. NILVs were harvested from cultured media and then concentrated by centrifuge as described above. The concentrated NILVs were titrated, aliquoted, and kept at -80 °C until use [54,55,62].

NILVs expressing enhanced green fluorescence protein (EGFP, 1 μl, 5 × 10⁹ IU/ml) were intravitreally injected into 4-week-old mice; 5 days later, the eyeballs were isolated and fixed in 3.7 % formaldehyde for 2 h. Whole-mount retinas were blocked in 5 % normal goat serum for 30 min, stained overnight at 4 °C with isolectin B4 (IB4) (1:100 dilution (Thermo Fisher Scientific), a mouse endothelial cell marker [40]. Finally, the thoroughly-washed whole-mount retinas were subjected to photography in a confocal fluorescence microscope (Leica Microsystems Inc. Deerfield, IL, USA) [40,55].

Genomic editing of retinal cells in a mouse model of oxygen-induced retinopathy

This experiment was performed as described previously [40,47]. Briefly, C57BL/6J litters on postnatal day (P) 7 were exposed to 75 % O₂ until P12 in an oxygen chamber (Central South University,

Changsha, China). At P12, the anesthetized pups were intravitreally injected with NILVs-LV5 and NILVs-LV6 (PE6x) targeting *VEGFR2* or *lacZ* (1 μl, 5.0 × 10⁹ vg/ml). After injection, the eyes were treated with a triple antibiotic (Neo/Poly/Bac) ointment and kept in room air (21 % O₂). At P17, the mice were euthanized, and retinas were carefully removed for Western blot analysis, NGS or fixed in 3.7 % paraformaldehyde. Mice under 6 g of total body weight were excluded from the experiments. Each experiment was at least repeated 2 times with more than 6 mice at each treatment in this OIR model. Retinal whole-mounts were stained overnight at 4 °C with IB4-Alexa 594 (red). The images were taken in the Leica confocal fluorescence microscope.

Examination of toxicity of PE6x-VEGFR2 in mouse eyes

6-weeks-old C57BL/6J mice were anesthetized and intravitreally injected with 1 μl (5.0 × 10⁹ vg/ml) of NILV-LV5 and NILV-LV6 (PE6x) targeting *VEGFR2* or *lacZ*. After 4 weeks of injection, electroretinography (ERG) (by light/dark adaptation) (Roland, Heidelberger Straße, Germany), optical coherence tomography (OCT) and fundus fluorescein angiography (FFA) were conducted using a Micron IV image system (Phoenix-Micron, Inc, Bend, OR, USA) as described previously [40,58] and in brief below.

OCT. When mice were deeply anesthetized with an intraperitoneal injection of ketamine/xylazine (100–200 mg/kg Ketamine/20 mg/kg Xylazine), their pupils were dilated with topical 1 % Tropicamide, and their eyes were covered with Genteal gel to prevent drying of the cornea. The fundus camera in the optical head of the apparatus provided initial alignment, and final alignment was guided by monitoring the real time OCT image of the retina.

ERG. After overnight dark adaptation, mice were examined under dim red light for ERG. Under anesthesia, their pupils were dilated and eyes covered with Genteal. Subsequently, a drop of 0.9 % sterile saline was put on the cornea of the treated eye to prevent dehydration and to allow electrical contact with the recording electrode (gold wire loop). A 25-gauge platinum needle, inserted subcutaneously in the forehead, served as reference electrode, while a needle inserted subcutaneously near the tail served as the ground electrode. A series of flash intensities was produced by a Ganzfeld controlled by the Diagnosys Espion 3 to test both scotopic and photopic response.

FFA. After animals were anesthetized their pupils were dilated, a drop of sterile saline was placed on the experimental eye to remove any debris followed by Genteal. Then 0.01 ml of 25 % sodium fluorescein (pharmaceutical grade sodium fluorescein; Akorn Inc) 5 g body weight was injected intraperitoneally. The retinal vasculature was filled with dye in less than one min following injection. Photos were taken sequentially at 1 and 5 min post fluorescein injection.

After mice were examined by OCT, ERG and FFA, they were euthanized, and their eyeballs were carefully removed and fixed in 3.7 % paraformaldehyde (PFA) for histological analysis as described previously [40,58].

All animal experiments followed the guidelines of the Association for Research in Vision and Ophthalmology Statement for the Use of Animals in Ophthalmic and Vision Research. Investigators who conducted analysis were masked as to the treatment groups. All the mice were cared for by following the ACUC protocol approved by the Institutional Animal Ethics Committee of Peking University at Shenzhen (Shenzhen, China).

Statistics

The data from 3 independent experiments were analyzed using an unpaired *t*-test between two groups, and one-way ANOVA

among more than two groups. For animal experiments the data from at least 6 mice were used for the statistical analysis. All data were analyzed using a masked procedure. P values < 0.05 were considered statistically significant.

Ethics statement

All experiments involving animals were conducted according to the ethical policies and procedures approved by the Animal Ethics Committee of Peking University at Shenzhen (Approval no. AP-2021-04).

Results

Creation of a dual NILV system for delivering PE6x

Lentiviral vectors (LVs) can transport large nucleotide fragments and preferentially transduce transcriptionally active cells including vascular endothelial cells (ECs) in the neo-vascular network [37,63,64,65]. Retinal photoreceptor cells are permanently differentiated cells and thus are difficult to be targeted by LVs [37,63,64,65], indicative of that the retinal neural cells are potentially protected when a NILV is employed as a gene editing vector for treating pathological intraocular angiogenesis such as PDR. We therefore aimed to develop a dual NILV system (Fig. 1A) for delivering PE6x intravitreally to create a T17967A mutation at the *Mus musculus VEGFR2* locus (NC_00071.6), resulting in a generation of an earlier stop codon (TAG, K796stop) from AAG (K796) when *VEGFR2* was transcribed and spliced in ECs during pathological angiogenesis (Fig. 1B). We envisioned that a dominant-negative (DN) VEGFR2 with 795 amino acids (aa) would be produced during translation as a result of the PE6x-generated stop codon (K796stop), which is located at an intracellular juxtamembrane domain (Fig. 1C), and that this DN-VEGFR2 will block VEGF/VEGFR2 signaling and hereby dampen pathological retinal angiogenesis.

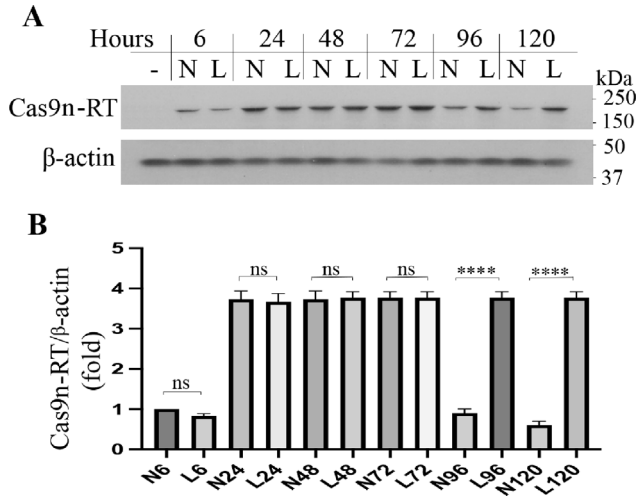


Fig. 2. Expression of Cas9n-RT delivered by NILV is transient in mouse vascular endothelial cells. **A.** Western blotting analysis of clarified lysates from mouse vascular endothelial cells (MVECs) infected by non-integrated lentivirus (NILV: N) or lentiviruses (LV: L), which carried a fusion protein of SpCas9n (Cas9n) with enhanced reverse transcriptase (RT). **B.** Quantification of western blotting band intensity. Data were from 3 representative independent experiments. N6 and L6: infection for 6 h; N120 and L120: infection for 120 h; ns: not significant; ****: significant with $p < 0.0001$ using one-way ANOVA.

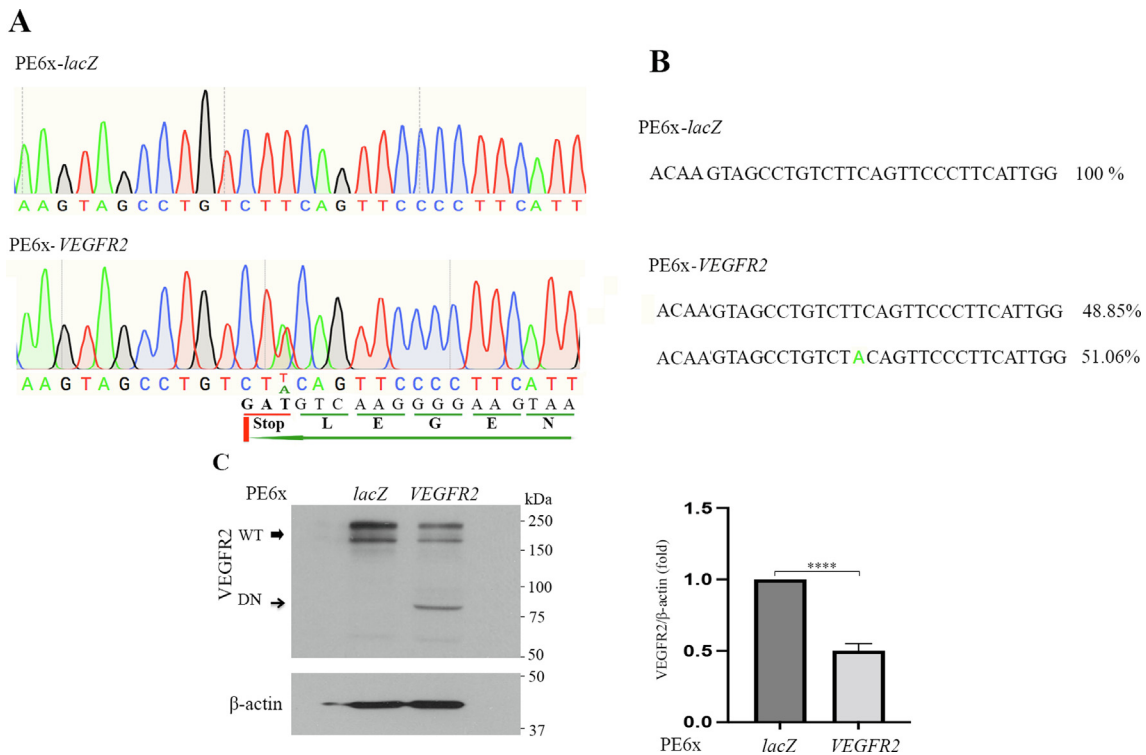


Fig. 3. Generation of dominant negative VEGFR2 by prime editing in vitro. **A.** Sanger DNA sequencing analysis of PCR products from genomic loci of MVECs transduced by dual NILVs, which carried a PE6x system consisting of 1) a fusion protein of SpCas9n with enhanced reverse transcriptase (RT) and epegRNA targeting *lacZ* (as a control) or *VEGFR2*, and 2) MLH1dn and nicking sgRNA targeting *lacZ* (as a control) or *VEGFR2*. There is a point mutation in genomic DNA transduced by PE6x-targeting *VEGFR2* (PE6x-*VEGFR2*), Stop: stop codon (TAG). **B.** Next generation sequencing (NGS) analysis of PCR products from genomic loci of MVECs in A. **C.** Western blotting analyses of lysates from transduced MVECs with indicated antibodies. A representative image shown on the left, and bar graphs were the data of western blot band intensity (VEGFR2 versus β -actin) from 3 representative experiments shown on the right; ****: significant with $p < 0.0001$ using an un-paired *t* test.

Among the dual NILV system, LV5 was created to express a fusion protein of SpCas9n (H840A) with a codon-optimized RT driven by an EF1 α core promoter and an epegRNA with a structured RNA sequence (TevopreQ1) driven by a U6 promoter [21,56], and LV6 was to express a dominant-negative MLH1 (MLHdn) [24] and a nicking sgRNA (ngRNA) (Fig. 1A-B). To this end, three vectors: 1) LV5 or LV6 with an desired epegRNA or a ngRNA [56] targeting genomic *VEGFR2* or a bacterial gene *lacZ* as a control; 2) an integrase-deficient packaging vector expressing the genes of *Gag* and *Pol* encoding RT and integrase with a D64V mutation to inactivate it [50]; and 3) one expressing the VSV (vesicular stomatitis virus)-G protein [59], were together transfected into HEK293T cells for producing NILVs. NILV5 and NILV6 (Fig. 1A) were then concentrated and titrated for *in vitro* and *in vivo* use.

Generation of a dominant-negative *VEGFR2* by PE6x *in vitro*

To assess if the dual NILV system was expressed transiently, we infected C57BL/6 mouse primary brain microvascular endothelial cells (MVECs) [40] with NILV5 or wild type (WT) LV5 for varying periods, and their lysates were subjected to a western blot analysis.

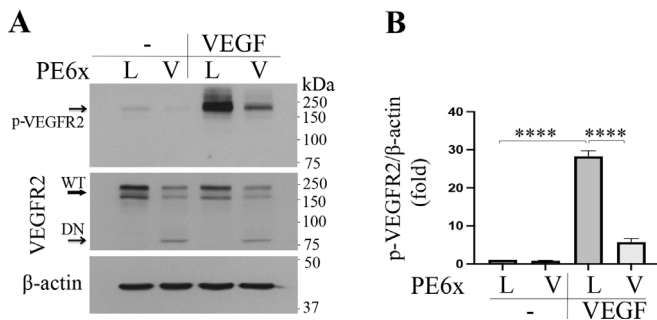


Fig. 4. PE6x-created dominative-negative *VEGFR2* attenuates VEGF-induced *VEGFR2* activation *in vitro*. A. Western blotting analysis of lysates from mouse vascular endothelial cells, which were transduced by NILV-PE6x targeting *VEGFR2* or *lacZ* as a control, and stimulated by VEGF-A for 10 min after growth factors-deprivation. A representative image was shown. L: *lacZ*, V: *VEGFR2*. B. Bar graphs were the data of western blot band intensity (p-VEGFR2 versus β-actin) from 3 representative experiments; ****: significant with $p < 0.0001$ using an un-paired *t* test.

As shown in Fig. 2, expression of a fusion protein with SpCas9n was detected at 6 h after NILV5 infection, and it reached the maximal at 48 h, which was maintained until 72 h after infection, and then dropped 51.2 ± 2.6 % down at 96 h, whereas SpCas9n/RT was kept to the almost same levels at this time when infected by WT LV5, indicating that SpCas9n/RT in PE6x is transiently expressed when cells are infected by the dual NILV system.

To explore whether DN-*VEGFR2* was produced by PE6x, we infected MVECs with the dual NILV system of NILV5 and NILV6 targeting genomic *VEGFR2* or its control gene *lacZ* (Fig. 1). On day 3 after infection, genomic DNA and proteins isolated from the infected MVECs were subjected to PCR and western blot analyses, respectively. Sanger DNA sequencing of the PCR products showed that there was a T17967A mutation at the *VEGFR2* locus (Fig. 3A), and next generation sequencing (NGS) demonstrated that the T17967A reached 51.06 % among the PCR-amplified genomic fragments from the MVECs infected by the dual NILVs (Fig. 3B). This point mutation was designed to alter **AAG** (K796) to **TAG** (Stop codon), resulting in generation of DN-*VEGFR2* by the dual NILV system (Fig. 1). Western blot analysis revealed that there was a smaller *VEGFR2* fragment appeared with a molecular weight of around 88 kDa (kDa), with the level of WT *VEGFR2* reduced 45.2 ± 3.6 % in the MVECs infected by the dual NILV system targeting *VEGFR2* compared with those targeting *lacZ* (Fig. 3C). These results demonstrate that the T17967A mutation created by the PE6x in the genomic DNA of MVECs results in termination of translation of the whole-length *VEGFR2* mRNA at the earlier stop codon, and thus production of a new truncated protein: DN-*VEGFR2* (88 kDa), as well as a decrease in WT *VEGFR2* expression.

DN-*VEGFR2* generated by PE6x blocks VEGF-induced *VEGFR2* activation

DN-proteins can inhibit the function of their respective WT counterparts [24,66–71]. We therefore next interrogated whether the DN-*VEGFR2* generated by PE6x could block the activity of WT *VEGFR2*, which is essential for angiogenesis [13,40,69–71]. To answer this question, MVECs infected by the dual NILV system on day 3 were treated in the presence or absence of VEGF (10 ng/ml) for 10 min, and lysates subjected to a western blot analysis, which revealed that DN-*VEGFR2* reduced *VEGFR2* phosphorylation on Y951 by 79.8 ± 3.5 % (Fig. 4).

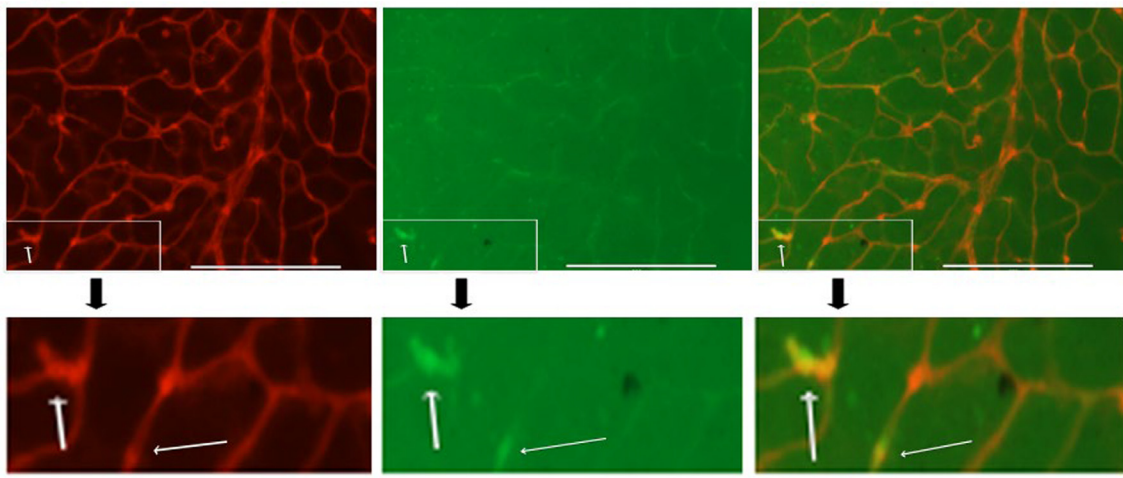


Fig. 5. NILVs transduce vascular endothelial cells *in vivo*. NILVs expressing EGFP ($1 \mu\text{l}$, 5×10^9 IU/ml) were intravitreally injected into 4-week-old mice; 5 days later, the eyeballs were isolated and whole-mount retinas were stained with IB4, a mouse endothelial cell marker. The stained whole-mount retinas were photographed in a fluorescence microscope. Black thick arrows: amplification of square areas; thin white arrows: representative merge of GFP with IB4, scale bar: 200 μm.

DN-VEGFR2 generated by PE6x impedes pathological retinal angiogenesis in a mouse model of oxygen-induced retinopathy

Encouraged by the cell-based observation above, we next sought to examine whether DN-VEGFR2 could be generated by PE6x *in vivo* to inhibit retinal angiogenesis in a mouse model of OIR. First, we assessed if NILV could infect retinal vascular ECs *in vivo* by intravitreal injection of NILV carrying CMV-GFP (NILV-GFP) into mice around 4-week-old. Whole-mount retinas from the mice at day 5 after injection were stained with isolectin 4 (IB4), a mouse endothelial specific marker. The results showed that GFP signal was co-localized with IB4 in whole-mount retinas in the NILV-GFP injected mice (Fig. 5A), indicating that NILVs are capable of transducing retinal vascular ECs.

We then intravitreally injected equal amounts of NILV5 and NILV6 targeting murine *VEGFR2* or *lacZ* into P12 mouse eyes within the OIR model. In this model, P7 mice are placed in a hyperoxic

(75 % oxygen) chamber for 5 days, during which central retinal vessel growth is inhibited; P12 mice are then returned to normal room air (21 % oxygen). From this time, relative hypoxia induces central normal vessel regrowth and peripheral retinal abnormal angiogenesis, which is termed as preretinal tufts, which reach a maximal at P17. Whole-mount retinas from the P17 mice injected with PE6x targeting *VEGFR2* or *lacZ* were stained with IB4. As shown in Fig. 6, there was a 93.5 ± 2.1 % reduction in IB4-stained peripheral tufts and a 63.6 ± 3.2 % decrease in the central retinal regrowth in mice injected with the dual NILVs targeting *VEGFR2* compared to those targeting *lacZ*, demonstrating that DN-VEGFR2 generated by PE6x in retinal vascular ECs impedes hypoxia-induced retinal angiogenesis in the mouse model of OIR.

To validate this speculation, the genomic DNA and proteins from the treated mouse retinas were subjected to next generation sequencing (NGS) and western blot analyses, respectively. The NGS results showed that there was about 11.77 % of T17967A mutation

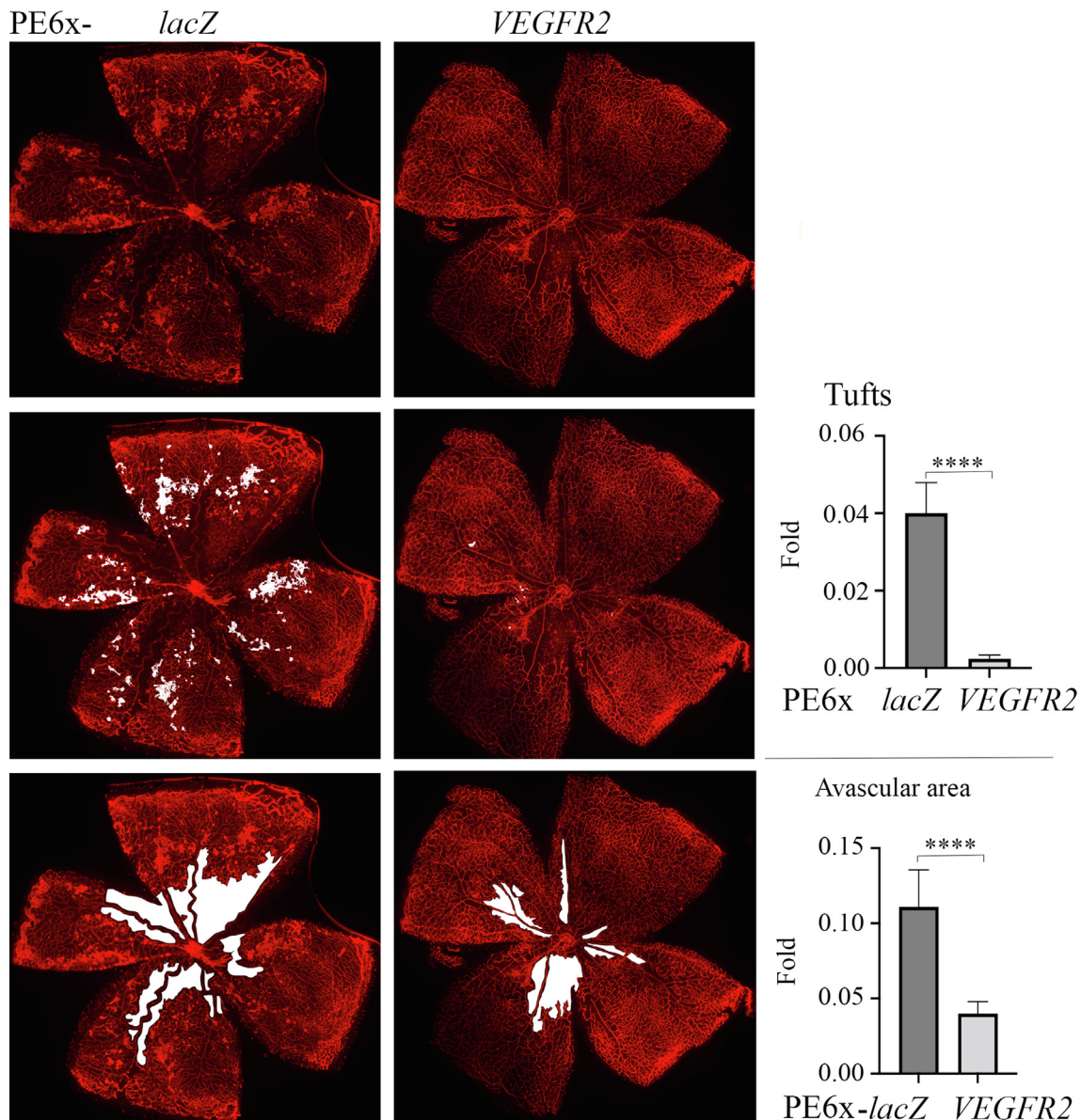


Fig. 6. DN-VEGFR2 generated by PE6x impedes pathological retinal angiogenesis in a mouse model of oxygen-induced retinopathy Representative of IB4 staining analysis of retinal neovascularization in P17 mice of OIR after intravitreal injection of NILV-PE6x targeting *VEGFR2* or *lacZ* into P12 OIR mice (left). Bar graphs were the data of IB4-stained retinas (n = 6) from mice intravitreally injected with NILV-PE6x targeting *VEGFR2* or *lacZ*. ****: significant with $p < 0.0001$ using an un-paired *t* test.

from genomic DNA of the retinas treated with the dual NILVs targeting *VEGFR2*, but none with targeting *lacZ* (Fig. 7A); western blotting analysis results demonstrated that there were a smaller *VEGFR2* protein appearing as well as a $22.6 \pm 2.5\%$ reduction in *VEGFR2* from mice injected with the dual NILVs targeting *VEGFR2* compared to those targeting *lacZ* (Fig. 7B). Collectively, these data demonstrate that DN-*VEGFR2* can be generated in genomic *VEGFR2* using PE6x *in vivo* and this DN-*VEGFR2* is sufficient to block hypoxia-induced angiogenesis in the mouse model of OIR.

Notably, the dual NILVs targeting genomic *VEGFR2* did not cause detectable damage to the retinal morphology, structure, and function examined by histological staining with hematoxylin & eosin, OCT, ERG, and FFA at 4-weeks after intravitreal injection in adult mice (Fig. 8).

Discussion

In this article we document that a retinal *VEGFR2* T17967A mutation created by editing genomic *VEGFR2* locus with PE6x results in generation of an earlier stop codon (TAG, K796stop) and thus a retinal DN-*VEGFR2* to block retinal *VEGFR2* expression and activity as well as abnormal retinal angiogenesis in the mouse model of OIR. This PE6x system was delivered to retinas using dual NILVs via intravitreal injection. Retroviral delivery of DN-*VEGFR2* directly into animal models has been shown to suppress tumor angiogenesis [69,70] and wound angiogenesis [71]. These prior investigations established a foundation for us to employ NILVs to deliver PE6x, an advanced PE system, for editing a genomic *VEGFR2* locus to produce an endogenous DN-*VEGFR2*, leading to inhibition

A

PE6x-*LacZ*

ACAA GTAGCCTGTCTTCAGTTCCTTCATTGG 100%

PE6x-*VEGFR2*

ACAA GTAGCCTGTCTT CAGTTCCTTCATTGG 88.16%

ACAA GTAGCCTGTCT A CAGTTCCTTCATTGG 11.77%

B

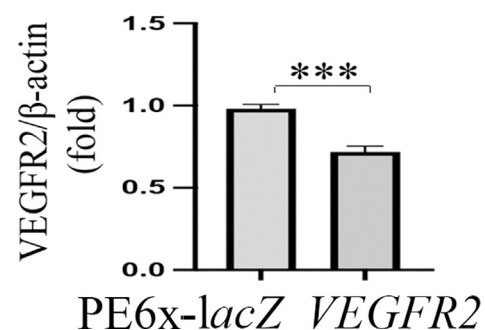
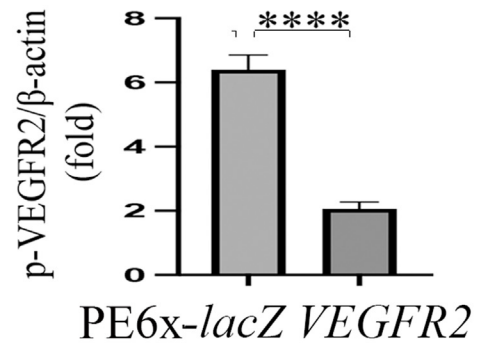
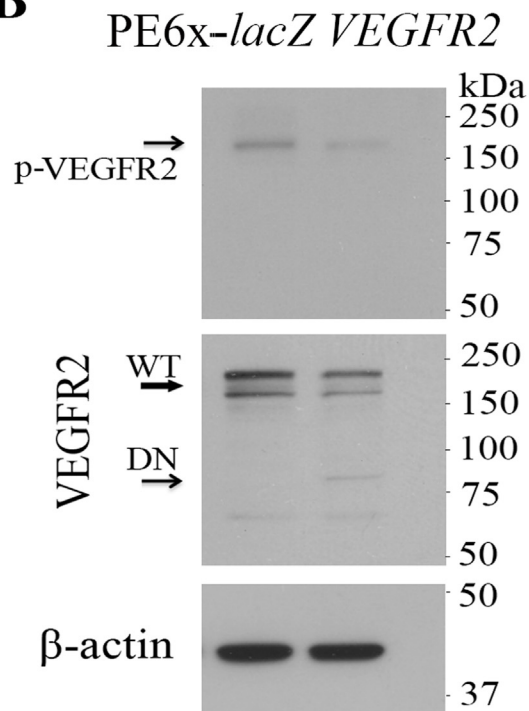


Fig. 7. Generation of *VEGFR2* T17967A and DN-*VEGFR2* by PE6x *in vivo* A. NGS analysis of genomic DNA from mouse retinas. A mutation of *VEGFR2* T17967A (K796stop) was generated in retinas from P17 OIR mice after intravitreal injection of NILV-PE6x targeting *VEGFR2* or *lacZ* into P12 mice. B. Western blot analysis of retinal lysates with an antibody against N-terminal of *VEGFR2*. DN-*VEGFR2* was generated in P17 mouse retinas after intravitreal injection of NILV-PE6x targeting *VEGFR2* or *lacZ* into P12 OIR mice. Bar graphs were the data of western blot band intensity (p-*VEGFR2* or *VEGFR2* versus β -actin) from 3 representative experiments; *** and ****: significant with $p < 0.001$ and $p < 0.0001$, respectively, using an un-paired *t* test.

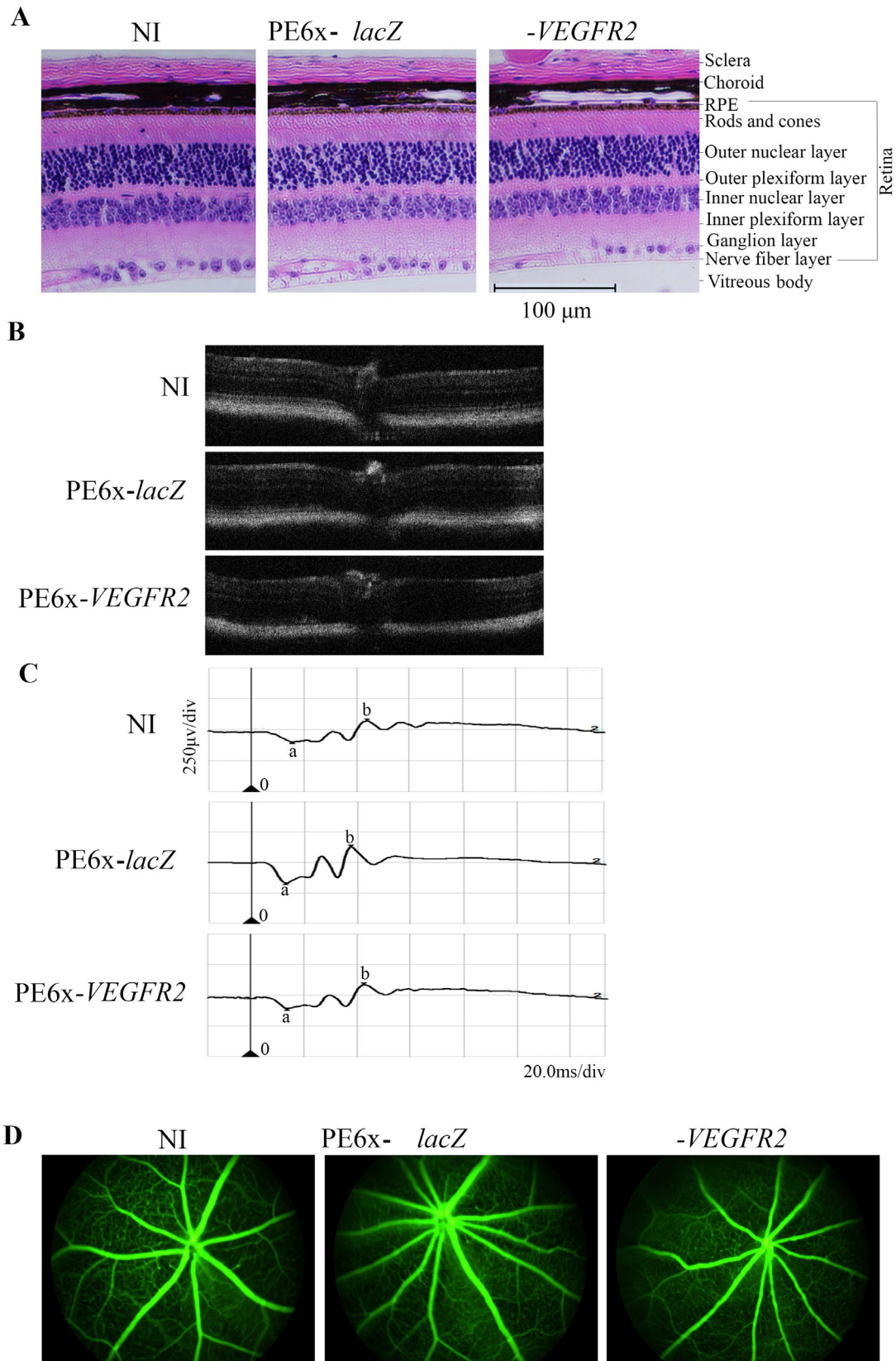


Fig. 8. Intravitreal injection of NILV-PE6x does not interfere with retinal structure and function 6-week-old mice were injected with the dual NILVs-PE6x targeting *VEGFR2* or *lacZ* into the left eye. After 4 weeks, the mice were examined by histology (H&E staining of eyeballs) (A), optical coherence tomography (OCT) (B), electroretinography (ERG) (C), and fundus fluorescein angiography (FFA) (D). NI: non-injection. PE6x-*lacZ*: dual NILVs targeting *lacZ*, PE6x-*VEGFR2*: dual NILVs targeting *VEGFR2*.

of retinal angiogenesis. In comparison with retrovirus, NILVs exhibit obvious advantages of safety due to its non-integrative behavior and higher infection efficiency. In particular, our aim here was to abrogate pathological retinal angiogenesis by intravitreal delivery of NILVs, which are localized in the eye and thus whose potential immunological response is limited due to ocular immune privilege [72–74]. Similarly, when anti-VEGF antibodies were first used to treat cancer patients received severe side effects due to requirement of VEGF for normal physiological activity [75–78], whereas these agents including ranibizumab and aflibercept are the current standard of care for numerous blinding eye diseases such as nAMD and PDR [79–81]. Thereby, our data provide strong support to leverage PE6x-generated DN-VEGFR2 as a novel strategy to treat intraocular angiogenesis including PDR.

Upon the advent of PE in 2019 [21], we transfected a PE2 system targeting genomic *VEGFR2* into 293 T cells, but the results showed that only 0.5 % edits were achieved (data not shown). This low editing efficiency might be due to an ineffective pegRNA or an MMR effect. When PE5 emerged in 2021 [24], we used a web tool [51] to design pegRNAs and then added a structured RNA motif tevpreQ₁ to its 3-terminus as epegRNAs to prevent their degradation [22]; furthermore, we also employed a nicking RNA to nick a non-edited strand [21] and a DN-protein to suppress MMR [24]. To our pleasant surprise, these optimized methods remarkably increased PE efficiency, reaching more than 50 % (Fig. 2A-B). Nevertheless, based on these results, we tried to further improve editing efficiency by modifying the lengths of PBS (Table 1), but these efforts did not lead to additional improvements (data not shown). Thereby, this dual-vector system for PE6x might be able to be generalized for broad applications.

Previous studies, which employed other gene editing strategies including AAV-mediated and endothelial specific promoter-driven SpCas9 targeting *VEGFR2* in the retina [40], lentiviral delivery of SpCas9 mRNA targeting *VEGF-A* in retinal pigment epithelial cells and AAV-mediated *Campylobacter jejuni* Cas9, a small Cas9) expression targeting *VEGF-A* [43], have been reported to inhibit intraocular angiogenesis in mouse models. Compared with these prior investigations prime editing is superior due to its non-breaking DNA double strands and thus increasing safety; compared with current intraocular anti-VEGF drugs, DN-VEGFR2 produced by prime editing may have higher efficiency in inhibiting angiogenesis due to its dual function of neutralizing VEGF and inhibiting VEGFR2 auto-phosphorylation. In addition, while anti-VEGF agents (e.g. ranibizumab and aflibercept) can suppress angiogenesis and vascular leakage associated with eye diseases (e.g. PDR and wet AMD), therapeutic challenges remain.

Notably, while genome editing strategies have their own advantages, they also bring their own set of limitations. For instance, it might result in certain degree of off-target effects and immune toxicity [44], which warrant further investigation when the PE6x is employed in clinical settings.

Conclusion

Our *in vitro* and *in vivo* work presented in this article demonstrates that PE6x-mediated expression of DN-VEGFR2 provides a novel opportunity for treating aberrant intraocular angiogenesis including PDR. Nonetheless, it is intriguing to explore whether this strategy can be harnessed to inhibit angiogenesis in other animal models (e.g., tumor angiogenesis, laser-induced choroid neovascularization). For these efforts will be necessary to expand its applications.

Compliance with ethics

All the animal experiments followed the guidelines of the Association for Research in Vision and Ophthalmology Statement for the Use of Animals in Ophthalmic and Vision Research. Investigators who conducted analysis were masked as to the treatment groups. All experiments involving animals were conducted according to the ethical policies and procedures approved by the laboratory animal ethics committee of Peking University at Shenzhen (Approval no. AP-2021-04).

Credit author statement

X.H., W.W. and H.Q., performed DNA preparation, cell culture, lentivirus production and infection, genomic DNA isolation, intravitreal injection, Western blot, whole mount retinal staining, analysis of the results, and wrote the manuscript; X.Y., L.D., Y.Y. and Q.Z. assisted on the *in vitro* and *in vivo* experiments; G.M., G.Z., and H.L. acquired funds, conceived the experiments, analyzed the data and revised the manuscript. All the authors reviewed the manuscript.

Declaration of competing interest

The authors declare that they have no known competing financial interests or personal relationships that could have appeared to influence the work reported in this paper.

Acknowledgements

We thank Professor Bart Vanhaesebroeck at University College London for carefully editing this paper. Dr. Hetian Lei is the guarantor of this work, and has full access to all the data in the study and takes responsibility for the integrity of the data and the accuracy of the data analysis.

Finance Disclosure

This work was supported by National Natural Science Foundation of China (82070989 to H.L.), the Research Foundation of Science and Technology Plan Project, Shenzhen (SGDX20211123120001001 and JCYJ20200109145001814 to X.Y. and H.L.), National Natural Science Foundation of China (82160199 to X.H., 82271109 to WW and 82271103 to G.Z.), Foreign Expert Project of Hainan Province (G20241024015E to H.L. and X.H.), Hainan Provincial Natural Science Foundation of China (821RC1126 to X.H.), Major program of Medical Science challenging plan of Henan province (SBGJ202102190 to G.M.), Introduction plan of high-level foreign experts (G2022026027L to G.M. and H.L.), and Guangdong Provincial Natural Science Foundation of China (2022A1515012326 to G.Z.). No funding bodies had any role in study design, data collection and analysis, decision to publish, or preparation of the manuscript.

References

- [1] Senger DR, Galli SJ, Dvorak AM, Perruzzi CA, Harvey VS, Dvorak HF. Tumor cells secrete a vascular permeability factor that promotes accumulation of ascites fluid. *Science* 1983;219:983–5.
- [2] Shima DT, Adamis AP, Ferrara N, Yeo KT, Yeo TK, Allende R, et al. Hypoxic induction of endothelial cell growth factors in retinal cells: identification and characterization of vascular endothelial growth factor (VEGF) as the mitogen. *Mol Med* 1995;1:182–93.
- [3] Muller YA, Li B, Christinger HW, Wells JA, Cunningham BC, de Vos AM. Vascular endothelial growth factor: Crystal structure and functional mapping of the kinase domain receptor binding site. *Proc Natl Acad Sci U S A* 1997;94:7192–7.
- [4] Williams R, Airey M, Baxter H, Forrester J, Kennedy-Martin T, Girach A. Epidemiology of diabetic retinopathy and macular oedema: a systematic review. *Eye (Lond)* 2004;18:963–83.

- [5] Fraser-Bell S, Kaines A, Hykin PG. Update on treatments for diabetic macular edema. *Curr Opin Ophthalmol* 2008;19:185–9.
- [6] Mintz-Hittner HA, Kennedy KA, Chuang AZ. Group B-RC: Efficacy of intravitreal bevacizumab for stage 3+ retinopathy of prematurity. *N Engl J Med* 2011;364:603–15.
- [7] Stahl A, Connor KM, Sapieha P, Chen J, Dennison RJ, Krah NM, et al. The mouse retina as an angiogenesis model. *Invest Ophthalmol Vis Sci* 2010;51:2813–26.
- [8] Chakravarthy U, Harding SP, Rogers CA, Downes SM, Lotery AJ, Culliford LA, et al. investigators I: Alternative treatments to inhibit VEGF in age-related choroidal neovascularisation: 2-year findings of the IVAN randomised controlled trial. *Lancet* 2013;382:1258–67.
- [9] Holmes K, Roberts OL, Thomas AM, Cross MJ. Vascular endothelial growth factor receptor-2: Structure, function, intracellular signalling and therapeutic inhibition. *Cell Signal* 2007;19:2003–12.
- [10] Sun J, Huang W, Yang SF, Zhang XP, Yu Q, Zhang ZQ, et al. Galphai1 and Galphai3 mediate VEGF-induced VEGFR2 endocytosis, signaling and angiogenesis. *Theranostics* 2018;8:4695–709.
- [11] Hegde M, Guruprasad KP, Ramachandra L, Satyamoorthy K, Joshi MB. Interleukin-6-mediated epigenetic control of the VEGFR2 gene induces disorganized angiogenesis in human breast tumors. *J Biol Chem* 2020;295:12086–98.
- [12] Shan HJ, Jiang K, Zhao MZ, Deng WJ, Cao WH, Li JJ, et al. SCF/c-Kit-activated signaling and angiogenesis require Galphai1 and Galphai3. *Int J Biol Sci* 2023;19:1910–24.
- [13] Kiselyov A, Balakin KV, Tkachenko SE. VEGF/VEGFR signalling as a target for inhibiting angiogenesis. *Expert Opin Investig Drugs* 2007;16:83–107.
- [14] Roodhart JM, Langenberg MH, Witteveen E, Voest EE. The molecular basis of class side effects due to treatment with inhibitors of the VEGF/VEGFR pathway. *Curr Clin Pharmacol* 2008;3:132–43.
- [15] Sharma PS, Sharma R, Tyagi T. VEGF/VEGFR pathway inhibitors as anti-angiogenic agents: Present and future. *Curr Cancer Drug Targets* 2011;11:624–53.
- [16] Uludag G, Hassan M, Matsumiya W, Pham BH, Chea S, Trong Tuong Than N, Doan HL, Akhavanrezaayat A, Halim MS, Do DV, Nguyen QD: Efficacy and safety of intravitreal anti-VEGF therapy in diabetic retinopathy: what we have learned and what should we learn further? *Expert Opin Biol Ther* 2022:1-17.
- [17] Arriago A, Aragona E, Bandello F. VEGF-targeting drugs for the treatment of retinal neovascularization in diabetic retinopathy. *Ann Med* 2022;54:1089–111.
- [18] Suzuki M, Nagai N, Izumi-Nagai K, Shinoda H, Koto T, Uchida A, et al. Predictive factors for non-response to intravitreal ranibizumab treatment in age-related macular degeneration. *Br J Ophthalmol* 2014;98:1186–91.
- [19] Raguram A, Banskota S, Liu DR. Therapeutic in vivo delivery of gene editing agents. *Cell* 2022.
- [20] Sheridan C. The world's first CRISPR therapy is approved: who will receive it? *Nat Biotechnol* 2023.
- [21] Anzalone AVRP, Davis JR, Sousa AA, Koblan LW, Levy JM, Chen PJ, et al. Search-and-replace genome editing without double-strand breaks or donor DNA. *Nature* 2019;576:149–57.
- [22] Nelson JW, Randolph PB, Shen SP, Everette KA, Chen PJ, Anzalone AV, et al. Engineered pegRNAs improve prime editing efficiency. *Nat Biotechnol* 2022;40:402–10.
- [23] Doman JL, Sousa AA, Randolph PB, Chen PJ, Liu DR. Designing and executing prime editing experiments in mammalian cells. *Nat Protoc* 2022;17:2431–68.
- [24] Chen PJ, Hussmann JA, Yan J, Knipping F, Ravisankar P, Chen PF, Chen C, Nelson JW, Newby GA, Sahin M, Osborn MJ, Weissman JS, Adamson B, Liu DR: Enhanced prime editing systems by manipulating cellular determinants of editing outcomes. *Cell* 2021, 184:5635–52 e29.
- [25] Doman JL, Pandey S, Neugebauer ME, An M, Davis JR, Randolph PB, McElroy A, Gao XD, Raguram A, Richter MF, Everette KA, Banskota S, Tian K, Tao YA, Tolar J, Osborn MJ, Liu DR: Phage-assisted evolution and protein engineering yield compact, efficient prime editors. *Cell* 2023, 186:3983–4002 e26.
- [26] Zheng C, Liang SQ, Liu B, Liu P, Kwan SY, Wolfe SA, et al. A flexible split prime editor using truncated reverse transcriptase improves dual-AAV delivery in mouse liver. *Mol Ther* 2022;30:1343–51.
- [27] Bosch JA, Birchak G, Perrimon N. Precise genome engineering in *Drosophila* using prime editing. *Proc Natl Acad Sci U S A* 2021;118.
- [28] Petri K, Zhang W, Ma J, Schmidts A, Lee H, Horng JE, et al. CRISPR prime editing with ribonucleoprotein complexes in zebrafish and primary human cells. *Nat Biotechnol* 2022;40:189–93.
- [29] Liu Y, Li X, He S, Huang S, Li C, Chen Y, et al. Efficient generation of mouse models with the prime editing system. *Cell Discov* 2020;6:27.
- [30] Liu P, Liang SQ, Zheng C, Mintzer E, Zhao YG, Ponniselvan K, et al. Improved prime editors enable pathogenic allele correction and cancer modelling in adult mice. *Nat Commun* 2021;12:2121.
- [31] Jiang T, Zhang XO, Weng Z, Xue W. Deletion and replacement of long genomic sequences using prime editing. *Nat Biotechnol* 2022;40:227–34.
- [32] Jang H, Jo DH, Cho CS, Shin JH, Seo JH, Yu G, et al. Application of prime editing to the correction of mutations and phenotypes in adult mice with liver and eye diseases. *Nat Biomed Eng* 2022;6:181–94.
- [33] Ely ZA, Mathey-Andrews N, Naranjo S, Gould SI, Mercer KL, Newby GA, et al. A prime editor mouse to model a broad spectrum of somatic mutations in vivo. *Nat Biotechnol* 2023.
- [34] Wang D, Zhang F, Gao G. CRISPR-based therapeutic genome editing: strategies and in vivo delivery by AAV vectors. *Cell* 2020;181:136–50.
- [35] Bulcha JT, Wang Y, Ma H, Tai PWL, Gao G. Viral vector platforms within the gene therapy landscape. *Signal Transduct Target Ther* 2021;6:53.
- [36] Leavitt AD, Robles G, Alesandro N, Varmus HE. Human immunodeficiency virus type 1 integrase mutants retain in vitro integrase activity yet fail to integrate viral DNA efficiently during infection. *J Virol* 1996;70:721–8.
- [37] Philippe S, Sarkis C, Barkats M, Mammeri H, Ladroue C, Petit C, et al. Lentiviral vectors with a defective integrase allow efficient and sustained transgene expression in vitro and in vivo. *Proc Natl Acad Sci U S A* 2006;103:17684–9.
- [38] Nightingale SJ, Hollis RP, Pepper KA, Petersen D, Yu XJ, Yang C, et al. Transient gene expression by nonintegrating lentiviral vectors. *Mol Ther* 2006;13:1121–32.
- [39] Mock U, Riecken K, Berdien B, Qasim W, Chan E, Cathomen T, et al. Novel lentiviral vectors with mutated reverse transcriptase for mRNA delivery of TALE nucleases. *Sci Rep* 2014;4:6409.
- [40] Huang X, Zhou G, Wu W, Duan Y, Ma G, Song J, et al. Genome editing abrogates angiogenesis in vivo. *Nat Commun* 2017;8:112.
- [41] Koo T, Park SW, Jo DH, Kim D, Kim JH, Cho HY, et al. CRISPR-LbCpf1 prevents choroidal neovascularization in a mouse model of age-related macular degeneration. *Nat Commun* 2018;9.
- [42] Wu W, Ma G, Qi H, Dong L, Chen F, Wang Y, et al. Genome editing of Pk3cd impedes abnormal retinal angiogenesis. *Hum Gene Ther* 2023;34:30–41.
- [43] Kim E, Koo T, Park SW, Kim D, Kim K, Cho HY, et al. In vivo genome editing with a small Cas9 orthologue derived from *Campylobacter jejuni*. *Nat Commun* 2017;8:14500.
- [44] Chen PJ, Liu DR. Prime editing for precise and highly versatile genome manipulation. *Nat Rev Genet* 2023;24:161–77.
- [45] An M, Raguram A, Du SW, Banskota S, Davis JR, Newby GA, et al. Engineered virus-like particles for transient delivery of prime editor ribonucleoprotein complexes in vivo. *Nat Biotechnol* 2024.
- [46] Davis JR, Banskota S, Levy JM, Newby GA, Wang X, Anzalone AV, et al. Efficient prime editing in mouse brain, liver and heart with dual AAVs. *Nat Biotechnol* 2023.
- [47] Connor KM, Krah NM, Dennison RJ, Aderman CM, Chen J, Guerin KI, et al. Quantification of oxygen-induced retinopathy in the mouse: a model of vessel loss, vessel regrowth and pathological angiogenesis. *Nat Protoc* 2009;4:1565–73.
- [48] Wu W, Zhou G, Han H, Huang X, Jiang H, Mukai S, et al. PI3Kdelta as a novel therapeutic target in pathological angiogenesis. *Diabetes* 2020;69:736–48.
- [49] Desjarlais M, Ruknudin P, Wirth M, Lahaie I, Dabouz R, Rivera JC, et al. Tyrosine-protein phosphatase non-receptor type 9 (PTPN9) negatively regulates the paracrine vasoprotective activity of bone-marrow derived pro-angiogenic cells: Impact on vascular degeneration in oxygen-induced retinopathy. *Front Cell Dev Biol* 2021;9:679906.
- [50] Certo MT, Ryu BY, Annis JE, Garibov M, Jarjour J, Rawlings DJ, et al. Tracking genome engineering outcome at individual DNA breakpoints. *Nat Methods* 2011;8:671–6.
- [51] Chow RD, Chen JS, Shen J, Chen S. A web tool for the design of prime-editing guide RNAs. *Nat Biomed Eng* 2021;5:190–4.
- [52] Matthews W, Jordan CT, Gavin M, Jenkins NA, Copeland NG, Lemischka IR. A receptor tyrosine kinase cDNA isolated from a population of enriched primitive hematopoietic cells and exhibiting close genetic linkage to c-kit. *Proc Natl Acad Sci U S A* 1991;88:9026–30.
- [53] Swiech L, Heidenreich M, Banerjee A, Habib N, Li Y, Trombetta J, et al. In vivo interrogation of gene function in the mammalian brain using CRISPR-Cas9. *Nat Biotechnol* 2015;33:102–6.
- [54] Huang X, Zhou G, Wu W, Ma G, D'Amore PA, Mukai S, et al. Editing VEGFR2 blocks VEGF-induced activation of Akt and tube formation. *Invest Ophthalmol Vis Sci* 2017;58:1228–36.
- [55] Wu W, Xia X, Tang L, Yao F, Xu H, Lei H. Normal vitreous promotes angiogenesis via activation of Axl. *FASEB J* 2021;35:e21152.
- [56] Sanjana NE, Shalem O, Zhang F. Improved vectors and genome-wide libraries for CRISPR screening. *Nat Methods* 2014;11:783–4.
- [57] Lei H, Qian CX, Lei J, Haddock LJ, Mukai S, Kazlauskas A. RasGAP promotes autophagy and thereby suppresses platelet-derived growth factor receptor-mediated signaling events, cellular responses, and pathology. *Mol Cell Biol* 2015;35:1673–85.
- [58] Dong L, Han H, Huang X, Ma G, Fang D, Qi H, et al. Idelalisib inhibits experimental proliferative vitreoretinopathy. *Lab Invest* 2022.
- [59] Stewart SA, Dykxhoorn DM, Palliser D, Mizuno H, Yu EY, An DS, et al. Lentivirus-delivered stable gene silencing by RNAi in primary cells. *RNA* 2003;9:493–501.
- [60] Salmon P, Trono D: Production and titration of lentiviral vectors. *Curr Protoc Hum Genet* 2007, Chapter 12:Unit 12.0.
- [61] Barde I, Salmon P, Trono D: Production and titration of lentiviral vectors. *Curr Protoc Neurosci* 2010, Chapter 4:Unit 4.21.
- [62] Lei H, Romeo G, Kazlauskas A. Heat shock protein 90alpha-dependent translocation of annexin II to the surface of endothelial cells modulates plasmin activity in the diabetic rat aorta. *Circ Res* 2004;94:902–9.
- [63] Schroder AR, Shinn P, Chen H, Berry C, Ecker JR, Bushman F. HIV-1 integration in the human genome favors active genes and local hotspots. *Cell* 2002;110:521–9.
- [64] Gruter O, Kostic C, Crippa SV, Perez MT, Zografos L, Schorderet DF, et al. Lentiviral vector-mediated gene transfer in adult mouse photoreceptors is impaired by the presence of a physical barrier. *Gene Ther* 2005;12:942–7.

- [65] Puppo A, Cesi G, Marrocco E, Piccolo P, Jacca S, Shayakhmetov DM, et al. Retinal transduction profiles by high-capacity viral vectors. *Gene Ther* 2014;21:855–65.
- [66] Wang XJ, Greenhalgh DA, Bickenbach JR, Jiang A, Bundman DS, Krieg T, et al. Expression of a dominant-negative type II transforming growth factor beta (TGF-beta) receptor in the epidermis of transgenic mice blocks TGF-beta-mediated growth inhibition. *Proc Natl Acad Sci U S A* 1997;94:2386–91.
- [67] Ikuno Y, Kazlauskas A. An in vivo gene therapy approach for experimental proliferative vitreoretinopathy using the truncated platelet-derived growth factor alpha receptor. *Invest Ophthalmol Vis Sci* 2002;43:2406–11.
- [68] Narayan V, Barber-Rotenberg JS, Jung IY, Lacey SF, Rech AJ, Davis MM, Hwang WT, Lal P, Carpenter EL, Maude SL, Plesa G, Vapiwala N, Chew A, Moniak M, Sebros RA, Farwell MD, Marshall A, Gilmore J, Lledo L, Dengel K, Church SE, Hether TD, Xu J, Gohil M, Buckingham TH, Yee SS, Gonzalez VE, Kulikovskaya I, Chen F, Tian L, Tien K, Gladney W, Nobles CL, Raymond HE, Prostate Cancer Cellular Therapy Program I, Hexner EO, Siegel DL, Bushman FD, June CH, Fraietta JA, Haas NB: PSMA-targeting TGFbeta-insensitive armored CAR T cells in metastatic castration-resistant prostate cancer: a phase 1 trial. *Nat Med* 2022, 28:724–34.
- [69] Machein MR, Risau W, Plate KH. Antiangiogenic gene therapy in a rat glioma model using a dominant-negative vascular endothelial growth factor receptor 2. *Hum Gene Ther* 1999;10:1117–28.
- [70] Stratmann A, Acker T, Burger AM, Amann K, Risau W, Plate KH. Differential inhibition of tumor angiogenesis by tie2 and vascular endothelial growth factor receptor-2 dominant-negative receptor mutants. *Int J Cancer* 2001;91:273–82.
- [71] Tsou R, Fathke C, Wilson L, Wallace K, Gibran N, Isik F. Retroviral delivery of dominant-negative vascular endothelial growth factor receptor type 2 to murine wounds inhibits wound angiogenesis. *Wound Repair Regen* 2002;10:222–9.
- [72] Zhou R, Caspi RR. Ocular immune privilege. *F1000 Biol Rep* 2010:2.
- [73] Taylor AW. Ocular immune privilege. *Eye (Lond)* 2009;23:1885–9.
- [74] Niederkorn JY. The eye sees eye to eye with the immune system: The 2019 proctor lecture. *Invest Ophthalmol Vis Sci* 2019;60:4489–95.
- [75] van Heeckeren WJ, Ortiz J, Cooney MM, Remick SC. Hypertension, proteinuria, and antagonism of vascular endothelial growth factor signaling: clinical toxicity, therapeutic target, or novel biomarker? *J Clin Oncol* 2007;25:2993–5.
- [76] Al-Husein B, Abdalla M, Trepte M, Deremer DL, Somanath PR. Antiangiogenic therapy for cancer: an update. *Pharmacotherapy* 2012;32:1095–111.
- [77] Kamba T, McDonald DM. Mechanisms of adverse effects of anti-VEGF therapy for cancer. *Br J Cancer* 2007;96:1788–95.
- [78] Chu TF, Rupnick MA, Kerkela R, Dallabrida SM, Zurakowski D, Nguyen L, et al. Cardiotoxicity associated with tyrosine kinase inhibitor sunitinib. *Lancet* 2007;370:2011–9.
- [79] Gragoudas ES, Adamis AP, Cunningham Jr ET, Feinsod M, Guyer DR. Group VISIONCT: Pegaptanib for neovascular age-related macular degeneration. *N Engl J Med* 2004;351:2805–16.
- [80] Broadhead GK, Keenan TDL, Chew EY, Wiley HE, Cukras CA. Comparison of agents using higher dose anti-VEGF therapy for treatment-resistant neovascular age-related macular degeneration. *Graefes Arch Clin Exp Ophthalmol* 2022;260:2239–47.
- [81] Ehlers JP, Yeh S, Maguire MG, Smith JR, Mruthyunjaya P, Jain N, et al. Intravitreal pharmacotherapies for diabetic macular edema: A report by the American Academy of Ophthalmology. *Ophthalmology* 2022;129:88–99.